

# Liquid Crystalline Azobenzene-Containing Polymer as a Matrix for Distributed Feedback Lasers

Leonid M. Goldenberg,<sup>\*,†,‡,§</sup> Victor Lisinetskii,<sup>\*,†</sup> Alexander Ryabchun,<sup>‡,§</sup> Alexey Bobrovsky,<sup>§</sup> and Sigurd Schrader<sup>†</sup>

<sup>†</sup>Technical University of Applied Sciences Wildau, Hochschulring 1, 15745 Wildau, Germany

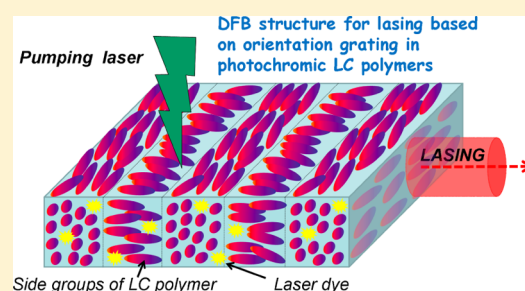
<sup>‡</sup>Fraunhofer Institute for Applied Polymer Research, Geiselbergstraße 69, 14476 Potsdam-Golm, Germany

<sup>§</sup>Faculty of Chemistry, Moscow State University, Leninskie Gory, 119991 Moscow, Russia

## Supporting Information

**ABSTRACT:** For the first time a liquid crystalline azobenzene-containing side-chain copolymer was employed as matrix material for distributed feedback lasers based on orientation gratings. Effective polarization gratings with periods of 245–290 nm could be inscribed within just one second using moderate light intensity. Using a number of near-infrared laser dyes and different grating frequencies, tuning of wavelength of the emitted radiation from 760 to 883 nm was obtained. It was also found that the lasing wavelength depends on the angle between the liquid crystal director and the grating vector. Wavelength tuning in the range of 30 nm was demonstrated using this method.

**KEYWORDS:** lasing, distributed feedback, polarization diffraction grating, liquid crystal, azobenzene, holography



Miniature organic waveguide-based lasers are promising devices for potential applications in photonics and sensorics.<sup>1,2</sup> One of the possible designs of such lasers is distributed feedback (DFB) lasers, where feedback is provided by a diffraction grating, which can be easily introduced into a slab waveguide of a laser. Recently a procedure for direct interference writing of gratings to produce miniaturized DFB lasers in a single optical step was established.<sup>3–7</sup> At the core of the approach is an ability of azobenzene-containing materials to build surface relief (SRG) and/or polarization gratings (in fact, refractive index gratings) under polarization interference exposure.<sup>8–10</sup> An azobenzene-containing epoxy oligomer was the first material used to show the proof of principle.<sup>3,4</sup> The material is characterized by a very fast rate of SRG inscription and rather moderate photoinduced birefringence.<sup>9</sup> Further, application of polarization gratings was extended to other amorphous side-chain azobenzene-containing polymers.<sup>6,7</sup> These materials allowed extending the wavelength tuning range over 200 nm and increased the device stability. While SRG was successfully applied until now only to epoxy oligomers<sup>3,5</sup> due to this material's high rate of SRG inscription,<sup>5</sup> application of polarization gratings seems to be a more general approach, which already is implemented in three different azobenzene matrices.<sup>4,6,7</sup> This fact is due to the trade-off between efficient DFB structure inscription and emitter (laser dye, for instance) bleaching by light during the holographic exposure. The rate of SRG inscription of different azobenzene-containing materials differs considerably;<sup>11</sup> therefore writing of sufficient DFB structure without fluorophore bleaching would be possible only in rather fast materials. For example fabrication

of lasers based on SRG in amorphous azobenzene polyelectrolyte PAZO was not possible due to the moderate rate of SRG inscription,<sup>3</sup> but was rather successful using polarization gratings.<sup>6</sup> On the other hand, many (but not all) azobenzene-containing materials possess the ability of stable photoinduced orientation and, consequently, the ability of polarization grating inscription.<sup>8–10</sup> The photo-orientation phenomenon appears due to the cycles of *E*–*Z*–*E* photoisomerization of azobenzene chromophores followed by their rotational diffusion and alignment in perpendicular direction to the polarization of the excitation light. The efficiency of polarization grating inscription would definitely depend on the maximal value of the photoinduced birefringence. While materials with photoinduced birefringence up to 0.5 were reported,<sup>12–14</sup> even a birefringence on the order of 0.01 was sufficient to create refractive index gratings functioning as DFB structures for lasing.<sup>3</sup> This means that polarization gratings in azobenzene-containing materials (side-chain and main-chain polymers, molecular glasses, and supramolecular materials<sup>8–10</sup>) have significantly higher potential in comparison to SRG as DFB structures for lasing. As was already stated before,<sup>5–7</sup> the exploitation of a wealth of possible azobenzene-containing materials is the route for an improvement of laser performance parameters such as efficiency, stability, and tuning range. This could be of interest for application as miniature lasers<sup>1,2</sup> and for other applications of azobenzene-containing materials.<sup>15</sup>

Received: May 23, 2014

Published: August 7, 2014

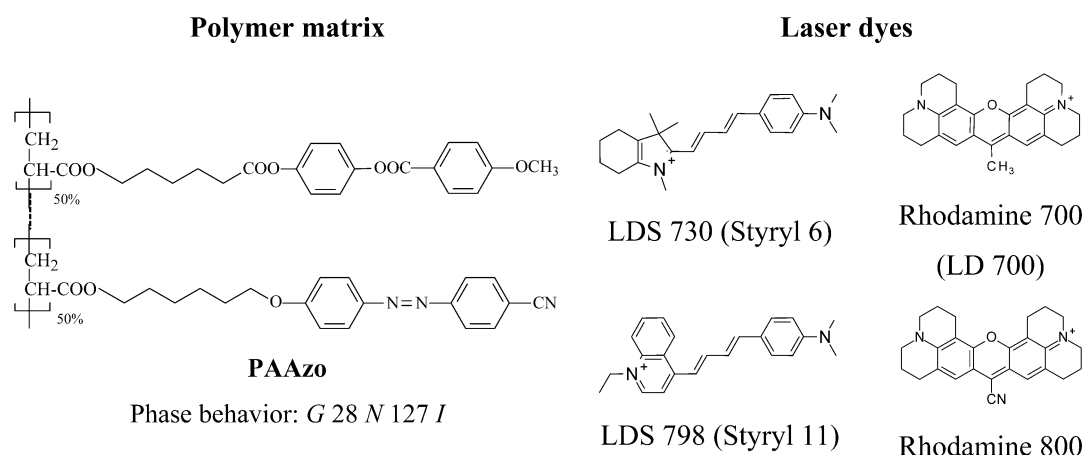


**Figure 1.** Chemical formula of used materials (G, glass state; N, nematic mesophase; I, isotropic melt).

One of the most attractive candidates for use as an effective material for polarization grating recording is liquid crystalline (LC) azobenzene-containing comb-shaped polymers.<sup>16–19</sup> Such materials combine the properties of polymers such as simple processability and high stability with liquid crystal features, such as high optical anisotropy and the ability to control properties by external fields, e.g., by light. Recently, a thin-film optical diode based on LC azobenzene-containing comb-shaped polymers was reported.<sup>19</sup>

Thereby the liquid crystalline copolymer PAAzo forming a nematic mesophase was selected as a polymer matrix for laser dye introduction (Figure 1). Such liquid crystalline azobenzene-containing polymers possess typically high thermal stability (up to 300 °C)<sup>20</sup> and a high light intensity threshold for photochemical degradation. An irradiation dose of up to 1000 J cm<sup>-2</sup> at 488 nm wavelength was used in polymers having chromophores of similar structure without noticeable azobenzene degradation.<sup>21</sup> PAAzo consists of azobenzene photochromic groups responsible for the *E–Z* isomerization, photoinduced orientation, and nonphotochromic nematogenic phenylbenzoate side groups. The homopolymer containing only azobenzene moieties of such structure forms a smectic phase suppressing the photo-orientation process.<sup>22</sup> Hence, in order to realize a less ordered nematic phase, a copolymer with an additional nematogenic phenylbenzoate side group was synthesized (the synthesis of monomers and copolymer was conducted by coauthors A.R. and A.B.). In addition, mesogenic groups introduced into the system enhance the refractive index modulation,<sup>23</sup> since the cooperative nature of the photoinduced orientation of both types of side groups is inherent to such material.<sup>24,25</sup>

Thus, we report here for the first time an application of a liquid crystalline azobenzene-containing polymer for a DFB single-layer laser device.

## EXPERIMENTAL PART

**Polymer Matrix Synthesis.** The copolymer PAAzo with a molar ratio of mesogenic and azobenzene side groups of 1:1 was synthesized by free radical polymerization of appropriate monomers that have been obtained according to procedures described elsewhere.<sup>26</sup> The reaction was carried out in anhydrous benzene in a sealed tube under an argon atmosphere with the initiator (AIBN, 2 wt %) for 100 h at 70 °C. The copolymer obtained was purified to get rid of low-molar-mass and oligomeric substances by prolonged treatment with boiling

methanol followed by drying in a vacuum at 50 °C for 2 h. The polymerization was carried out to high conversions. The  $M_w$  of PAAzo was about 8.6 kDa (degree of polymerization  $\sim$ 22, polydispersity  $\sim$ 1.55), which was determined by GPC using a Knauer chromatograph (UV detector, column type LC-100 with a sorbent 1000 Å; solvent THF, 1 mL/min; 25 °C; polystyrene standard). Phase transition temperatures were detected by a polarized optical microscope (POLAM-R-112) equipped with heating stage (Mettler FP-86), as well as differential scanning calorimetry (Mettler TA-4000, heating rate 10 K/min, samples were prepared as 5–10 mg tablets).

**Film Fabrication.** Rhodamine 700 (LD 700), Rhodamine 800 (LD 800), LDS 730, and LDS 798 (all Exciton) have been used as received. The nematic copolymer PAAzo obtained by the procedure described above was used as matrix material.

The films were spin-coated from 1,1,2-trichloroethane solutions onto soda lime glass substrates (refractive index 1.52, Carl Roth GmbH) with a rubbed polyimide (Nissan Chemical) coating. The laser dye was introduced into the material as guest (ca. 4% by weight) using the same 1,1,2-trichloroethane as a solvent. Films of PAAzo doped with laser dyes obtained by spin-coating from solutions do not form any LC phase due to fast solvent evaporation; that is, these freshly prepared films are amorphous. Hence, after spin-coating, the films were annealed at 80 °C for several hours in order to form a unidirectionally aligned monodomain nematic structure.

**Structuring.** The experimental setup (Figure 2) used for inscription of polarization gratings based on Lloyd's mirror interferometer has been described elsewhere.<sup>4–6</sup> The films were irradiated from the glass side with a polarization interference pattern formed by left- and right-handed circularly polarized light or with an intensity pattern formed by two beams of the

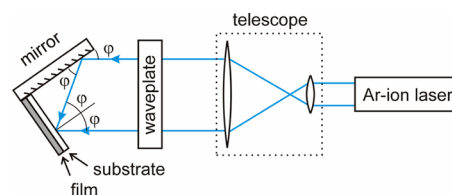


**Figure 2.** Experimental setup for inscription of polarization gratings. The waveplate is a quarter-wave plate for the inscription with circularly polarized beams and is a half-wave plate for the inscription with linearly polarized beams.

same linear polarization (vertical or horizontal). The pattern period ( $\Lambda$ ) and, hence, the period of the grating inscribed into the film were determined by the angle of incidence ( $\varphi$ , Figure 2) of light according to the following equation:

$$\Lambda = \frac{\lambda_0}{2 \sin(\varphi)} \quad (1)$$

where  $\lambda_0$  is the wavelength of the recording radiation. Radiation of a continuous-wave Ar-ion laser operating at 488 nm was used for this purpose. The intensity of each inscribing beam on the sample was ca. 140 mW cm<sup>-2</sup>. The angle of incidence ( $\varphi$ ) was chosen in the range 10–63.5°, resulting in pattern periods of 245–467 nm ( $\Lambda$ ). The absence of SRGs in the samples was proven by atomic force microscopy using a Veeco CPM microscope in the intermittent-contact mode. A typical sample image is presented in Figure S1.

The thickness of the samples was measured using a Veeco Dektak 150 profilometer. The value of the birefringence of the azobenzene polymers was obtained using the following method.<sup>10</sup> A film sample was exposed to vertically polarized radiation of the Ar-ion laser to induce uniaxial negative birefringence with a vertically oriented optical axis. Afterward, the sample was tested by a probe beam of a He–Ne laser linearly polarized at an angle of 45° to the vertical. The transmitted beam was analyzed with a system consisting of a half-wave plate and a Glan prism. Components polarized parallel to the polarization of the incoming beam ( $I_p$ ) and orthogonal to it ( $I_s$ ) were measured with a photodetector (Thorlabs DET100A). The induced birefringence ( $\Delta n$ ) was determined using the following equation:<sup>8</sup>

$$\Delta n = \frac{\lambda_{\text{HeNe}}}{\pi d} \arcsin \left( \sqrt{\frac{I_s}{I_s + I_p}} \right) \quad (2)$$

where  $\lambda_{\text{HeNe}}$  is the wavelength of the He–Ne laser (633 nm) and  $d$  is the thickness of the sample.

**Device Characterization.** The setup for investigation of lasing properties in the fabricated DFB structures was the same as in our previous papers.<sup>4–7</sup> A wavelength-tunable optic parametric oscillator (Continuum Surelite OPO Plus) was used as a pump source. The pump pulse duration was 3.5 ns, and the repetition rate was 10 Hz. A cylindrical lens focused the pump beam into a narrow stripe (5 mm length and 0.4 mm width) oriented along the grating vector. The radiation generated in the investigated samples was detected and investigated from an edge of a sample. The generation spectra were recorded with a Polytec Berlin AG (ETA-CS-HL) spectrometer, while for investigation of lasing stability a Polytec Berlin AG (BRC642E) spectrometer was used. The spectral resolution of both spectrometers was ca. 1.5 nm. The pump energy and the energy of output radiation were measured with a PEM 4 pyroelectric detector (energy meter LEM2020, Sensor- and Lasertechnik, Germany) and with a calibrated photodetector (Thorlabs DET100A).

## RESULTS AND DISCUSSION

The azobenzene-containing copolymer PAAzo forms a nematic mesophase with a clearing temperature of 127 °C with typical marble texture observed by polarized microscopy. According to DSC data, the glass transition temperature of the copolymer is about 28 °C.

Most of the mixtures with dyes were stable, and phase separation was not observed during prolonged storage even at elevated temperature. It was shown that the introduction of low-molar-mass laser dyes does not affect the mesophase type but leads to a reduction of the isotropization temperatures; for example, for a mixture of PAAzo + 4 wt % LD 700 the clearing point was 114 °C. This phenomenon can be explained by the nonmesogenic nature of the laser dyes disrupting the mesophase (low anisotropy of dye molecules).

The chemical formulas of the azobenzene-containing side-chain polymer and laser dyes successfully used as emitters are given in Figure 1.

**Measurements of Birefringence.** The birefringence of PAAzo was measured in the LC state after film formation on the rubbed polyimide substrate and was found to be 0.23. On the contrary no birefringence was detected for the amorphousized film (films without annealing) on the same rubbed substrate or on a glass substrate. Exposure of amorphousized films to linearly polarized light of 488 nm wavelength resulted in photoinduced birefringence of ca. 0.08–0.09. These values are smaller than the birefringence measured for films in the LC state (0.23). Hence, we can conclude that the order parameter in the irradiated amorphousized films is smaller than that of films in the LC state. This observation is in agreement with the previously published results obtained for similar azobenzene-containing polymers.<sup>22</sup>

The photoinduced birefringence in the LC films depends on the angle of the light polarization plane with respect to the rubbing direction. While azobenzene chromophores are oriented along the rubbing direction, exposure to light with polarization perpendicular to the rubbing direction did not lead to any change of birefringence. On the contrary, exposure to light with polarization parallel to the rubbing direction led to a decrease of birefringence to a value of 0.16. Additional measurements of the dependence of the film absorption on the light polarization showed that in the latter case azobenzene chromophores were oriented mainly orthogonal to the rubbing direction.

**Lasing Measurements.** We have tried a number of NIR laser dyes of Rhodamine and styryl type (Pyridine 1, Pyridine 2, DCM, DCM2, Rhodamine 700, Rhodamine 800, LDS 798, LDS 730). Some of these dyes (Pyridine 1, Pyridine 2, DCM, and DCM2) were incompatible with the LC matrix, forming scattering films. Consequently, amplified spontaneous emission (ASE) has been detected only for the last four NIR dyes (Figure 1); however, the lowest threshold value has been detected for Rhodamine 700. A significant difference has been observed between the ordered LC films on the rubbed substrates and the amorphousized films on conventional glass. The last ones exhibited a much higher ASE threshold due to the light scattering. Apparently, small LC domains were still present in the film, which led to light scattering (i.e., freshly prepared film was only partially amorphousized), notwithstanding that polarization optical microscopy did not reveal the presence of an LC phase by the multidomain LC structure.

Inscription of a polarization grating in a PAAzo polymer, doped with an emitter, resulted in a DFB laser device. In this device the polymer layer acts as both a light-guiding layer and active medium, while the grating inside provides a distributed feedback for lasing with a wavelength ( $\lambda_g$ ) obeying the Bragg condition:

$$m\lambda_g = 2n_{\text{eff}}\Lambda \quad (3)$$

where  $m$  is the order of the grating,  $\Lambda$  is the grating period, and  $n_{\text{eff}}$  is the effective refractive index, which can be determined by solving the waveguide characteristic equation.<sup>3–7</sup>

For all the investigated dyes, where ASE has been detected, DFB lasers emitting at a first diffraction order were obtained. Because the composition with a Rhodamine 700 dye showed the best lasing with lowest threshold, further detailed investigations were carried out for this composition only.

**Lasing in Amorphousized Films (PAAzo+Rh700).** Direct inscription of polarization gratings in amorphousized films did not result in DFB devices capable of lasing. Similarly to the case of ASE, this can be explained by light scattering due to the reason discussed above. This scattering both disturbs the holographic pattern formation during grating inscription and produces losses suppressing lasing.

Nevertheless, the fabrication of DFB lasers in amorphousized films turned out to be possible when the films have preliminary been illuminated with a linearly polarized Ar-laser radiation. For example, when the amorphousized film was irradiated with a light polarized along the  $z$ -axis (see Figure 3), fabrication of the first-order DFB laser with a grating vector along the  $x$ -axis was possible.

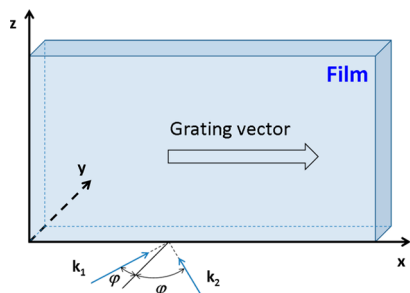


**Figure 3.** Presentation of the coordinate system used for description of holographic recording. The plane of the film is located in the  $xz$ -plane, and the grating vector is parallel to the  $x$ -axis;  $k_1$  and  $k_2$  are wave-vectors of interfering beams and are located in the  $xy$ -plane.

Typical generation spectra are presented in Figure 4.

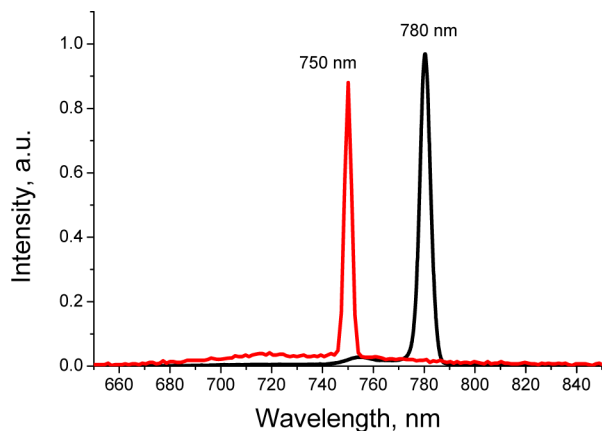


**Figure 4.** Lasing spectra of DFB structures fabricated in an amorphousized film (PAAzo+Rh700) oriented with vertically polarized light. The diffraction grating was written by two left- and right-handed circularly polarized beams (black line, grating period was 255 nm) and by two beams linearly polarized in the  $xy$ -plane (red line, grating period is 245 nm); the film thickness was ca. 800 nm.

It is interesting that in such oriented films a polarization grating can be written not only by interference of a left- and a right-handed circularly polarized beam (Figure 4, black line) but also by interference of two beams linearly polarized in the  $xy$ -plane (Figure 4, red line). This is not typical, as it is usually considered that gratings can be written effectively in azobenzene-based materials only by an interference pattern formed by a left- and a right-handed circularly polarized beam or by two beams of orthogonal linear polarization with a polarization plane at  $45^\circ$  forming the polarization interference pattern.<sup>8–10</sup> The effective refractive index of the films estimated in accordance with eq 3 is the same for both cases shown in Figure 4 and is about 1.53. The polarization of generated radiation was linear, corresponding to the TM mode of the waveguide. The generation threshold was ca.  $0.5 \text{ mJ cm}^{-2}$ . The possibility of diffraction grating inscription into the amorphousized film and the equality of the refractive indices for the cases under consideration can be explained as follows. After preliminary irradiation of the film with light polarized along the  $z$ -axis the LC domains are oriented in the  $xy$ -plane. First, the interaction of such a film with the interference pattern formed by a left- and a right-handed circularly polarized beam should be considered. Their electric fields ( $E_1$  and  $E_2$ ) can be expressed as follows:

$$\vec{E}_1(\vec{r}, t) = E_0 \cdot (\vec{e}_z \cos(\omega t - \vec{k}_1 \vec{r}) + (\vec{e}_x \cos \phi - \vec{e}_y \sin \phi) \times \sin(\omega t - \vec{k}_1 \vec{r})) \quad (4)$$

$$\vec{E}_2(\vec{r}, t) = E_0 \cdot (\vec{e}_z \cos(\omega t - \vec{k}_2 \vec{r}) - (\vec{e}_x \cos \phi + \vec{e}_y \sin \phi) \times \sin(\omega t - \vec{k}_2 \vec{r})) \quad (5)$$

where  $E_0$  is the amplitude of the electric field of each beam,  $\phi$  is the incidence angle,  $\omega$  is the circular frequency of light,  $t$  is a time coordinate,  $\vec{r} = x\vec{e}_x + y\vec{e}_y + z\vec{e}_z$  is a position vector, and  $\vec{k}_1$  and  $\vec{k}_2$  are the wave-vectors of the corresponding beams:

$$\vec{k}_1 = \frac{2\pi}{\lambda} (\vec{e}_x \sin \phi + \vec{e}_y \cos \phi),$$

$$\vec{k}_2 = \frac{2\pi}{\lambda} (-\vec{e}_x \sin \phi + \vec{e}_y \cos \phi) \quad (6)$$

Interference of these two waves in the plane of the film ( $\vec{r} = x\vec{e}_x + z\vec{e}_z$ ) results in the following electric field distribution:

$$\vec{E} = 2E_0 \cdot \left( \vec{e}_z \cos \omega t \cos\left(\frac{2\pi}{\lambda} \sin \phi x\right) - \vec{e}_x \cos \phi \cos \omega t \times \sin\left(\frac{2\pi}{\lambda} \sin \phi x\right) - \vec{e}_y \sin \phi \sin \omega t \cos\left(\frac{2\pi}{\lambda} \sin \phi x\right) \right) \quad (7)$$

For  $2\pi/\lambda \sin \phi x = \pi/2 + l\pi$ , where  $l$  is an integer number, the polarization of the electric field becomes linear oriented along the  $x$ -axis:

$$\vec{E} = 2E_0 \cdot \vec{e}_x \cos \phi \cos \omega t \quad (8)$$

For  $2\pi/\lambda \sin \phi x = l\pi$  the electric field (eq 7) is an elliptical polarization oriented in the  $yz$ -plane:

$$\vec{E} = 2E_0 \cdot (\vec{e}_z \cos \omega t - \vec{e}_y \sin \phi \sin \omega t) \quad (9)$$

Taking into account that the LC domains tend to be orthogonally oriented against the polarization of light, one can assume that for  $2\pi/\lambda \sin \phi x = l\pi$  the LC director is oriented

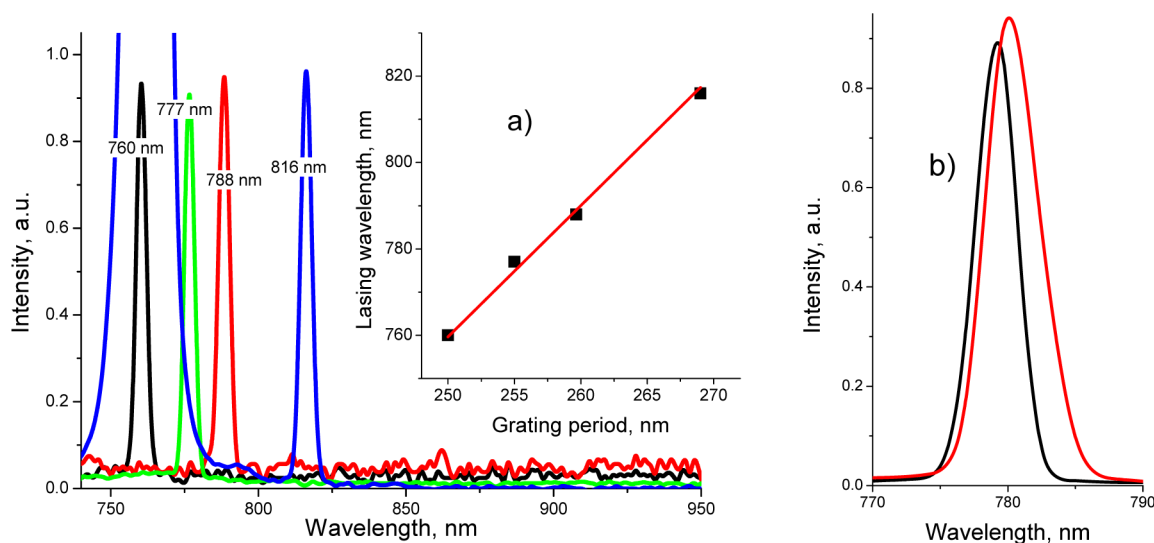


**Figure 5.** Lasing spectra of DFB structures (PAAzo+Rh700) with grating vector parallel to the LC director, pumped at 605 nm: (a) spectra of DFB structures with different grating periods (film thickness is 550 nm); the inset shows the corresponding dependency of the lasing wavelength on the grating period; (b) comparison of lasing spectra for DFB structures (film thickness is 800 nm) written with two circularly polarized beams (black line) and written with two beams linearly polarized in the  $xy$ -plane (red line).

along the  $x$ -axis. For  $2\pi/\lambda \sin \varphi x = \pi/2 + l\pi$  the LC domains are rotated to be orthogonal to the  $x$ -axis, but due to the initial distribution in the  $xy$ -plane, we can suppose that the domains are finally oriented along the  $y$ -axis.

In the case where the film is irradiated by two beams linearly polarized in the  $xy$ -plane the electric fields of the beams can be expressed as follows:

$$\vec{E}_1(\vec{r}, t) = E_0 \cdot (\vec{e}_x \cos \phi - \vec{e}_y \sin \phi) \sin(\omega t - \vec{k}_1 \vec{r}) \quad (10)$$

$$\vec{E}_2(\vec{r}, t) = -E_0 \cdot (\vec{e}_x \cos \phi + \vec{e}_y \sin \phi) \sin(\omega t - \vec{k}_1 \vec{r}) \quad (11)$$

Interference of these waves in the plane of the film provides

$$\begin{aligned} \vec{E} = & -2E_0 \cdot \left( \vec{e}_x \cos \phi \cos \omega t \sin\left(\frac{2\pi}{\lambda} \sin \phi x\right) \right. \\ & \left. + \vec{e}_y \times \sin \phi \sin \omega t \cos\left(\frac{2\pi}{\lambda} \sin \phi x\right) \right) \quad (12) \end{aligned}$$

Equation 12 shows that for  $2\pi/\lambda \sin \varphi x = \pi/2 + l\pi$  the electric field is oriented along the  $x$ -axis, while for  $2\pi/\lambda \sin \varphi x = l\pi$  the electric field is oriented along the  $y$ -axis. Taking into account that the LC domains are initially randomly distributed in the  $xy$ -plane and that they are rotated to be orthogonal to the electric field polarization one can conclude that the LC orientation is along the  $x$ -axis for  $2\pi/\lambda \sin \varphi x = l\pi$  and along the  $y$ -axis for  $2\pi/\lambda \sin \varphi x = \pi/2 + l\pi$ . The orientation is the same as that for the case of two circularly polarized beams. This explains the equality of the effective refractive indices for both cases.

Thus, in both considered cases LC domains are oriented sequentially along the  $y$ - and  $x$ -axis, forming regions with uniaxial positive birefringence with optical axes oriented along the  $y$ - and  $x$ -axis, respectively. When light propagates in a film along the  $x$ -axis (the direction of the grating vector), the TE mode (polarization is along the  $z$ -axis) is always the ordinary wave and there is no change of refractive index for this mode. The TM mode (polarization is along the  $y$ -axis) is the ordinary wave for the regions where the LC domains are oriented along

the  $x$ -axis and is the extraordinary wave for the regions where the LC domains are oriented along the  $y$ -axis. Designating the longitudinal component of the permittivity tensor of a LC domain as  $\varepsilon_p$  and the transversal component as  $\varepsilon_s$ , the difference between the minimum and maximum value of permittivity ( $\Delta\varepsilon$ ) for the TM mode can be expressed as follows:

$$\Delta\varepsilon = N_0(\varepsilon_p - \varepsilon_s) \quad (13)$$

where  $N_0$  is the relative number of oriented LC domains. The corresponding difference of the refractive indices was sufficiently high, and the TM mode was generated.

In the above-described case the grating vector was orthogonal to the polarization of light that was used for irradiation of the film before inscription of the grating. An inscription of a grating with grating vector parallel to the polarization did not result in any lasing. Cases of two left- and right-handed circularly polarized beams as well as two linearly polarized beams were tested with no success. Indeed, irradiation of the amorphousized film with light polarized along the  $x$ -axis distributes the LC domains in the  $yz$ -plane. Exposure of the film to an interference pattern formed by superposition of a left- and a right-handed circularly polarized beam (eq 7) results in a sequence of LC domains with orientation along the  $x$ -axis (for  $2\pi/\lambda \sin \varphi x = l\pi$ ) and in the  $yz$ -plane (for  $2\pi/\lambda \sin \varphi x = \pi/2 + l\pi$ ). This is the sequence of positive and negative birefringence with an optical axis along the  $x$ -axis, and both TM and TE modes of the film propagating along the  $x$ -axis are ordinary waves for all regions. The electric permittivity for these waves is equal to  $\varepsilon_{\perp}$  for a region where the LC director is parallel to the  $x$ -axis, while for a region where the LC directors are distributed in the  $yz$ -plane the permittivity can be expressed as  $N_0[(\varepsilon_p + \varepsilon_s)/2]$ . The resulting difference of permittivity is

$$\Delta\varepsilon = N_0 \frac{\varepsilon_p - \varepsilon_s}{2} \quad (14)$$

which is twice smaller than that in the case considered above (cf. eq 13). It is also possible to show that the same difference

of permittivity is created when the film oriented along the  $x$ -axis is irradiated with two linearly polarized beams. It seems that this difference could not provide a feedback sufficient for lasing in the presence of relatively high scattering by the LC domains.

**Lasing in Aligned Annealed Films (PAAzo+Rh700).** The case of annealed uniaxially oriented PAAzo polymer films in the LC state on a rubbed substrate is more complicated due to the presence of initial birefringence of the films. As a result, beams of Ar-laser radiation, which write the diffraction grating, are split into ordinary and extraordinary waves. These waves have different refractive indices and hence different angles of refraction in the films. The interference pattern cannot be described with eq 7 or 12; it is sufficiently more complicated and depends not only on the  $x$ -coordinate but also on the  $y$ -coordinate. Additionally, the LC layer, which is located close to the substrate surface, keeps the initial orientation even under exposure to light, and regions with biaxial anisotropy are formed.

In aligned films lasing on the first-order gratings was obtained for cases where the grating vector is parallel and perpendicular to the rubbing direction, respectively. Lasing spectra for the case with the grating vector parallel to the rubbing direction are presented in Figure 5a for different values of grating period. Tuning of the lasing wavelength in the range of 55 nm can be obtained. Fitting of these data with the formula for the Bragg condition (eq 3) yields an effective refractive index of ca. 1.52, which is close to that obtained for the above-described amorphous films. The difference can be attributed to the difference in thicknesses of the films (800 nm for the amorphous film and 550 nm for the oriented film).<sup>5</sup> Figure 5b shows generation spectra for a DFB laser written into the 800 nm thick film; the calculated effective index is 1.53. It should be noted that the increase of film thickness from 550 to 800 nm did not result in any change of generation threshold or efficiency. The gratings of DFB lasers (the spectra are shown in Figure 5a) were written with two circularly polarized beams. However, such a grating can also be written with two beams of linear polarization parallel to the rubbing direction. The generation spectrum of a DFB laser with a grating written in this way is also presented in Figure 5b (red line). The wavelength (780 nm) and the effective refractive index (1.53) are the same as for gratings recorded with two circularly polarized beams (Figure 5b, black curve). The lasing thresholds and efficiencies were also the same. In all these cases the output radiation was unpolarized.

It was found that an increase of the angle between grating vector and rubbing direction results in an increase of the generation wavelength. Typical lasing spectra for different values of the angle are presented in Figure 6. The dependence of the lasing wavelength on the angle is shown in the figure inset. Variation of the wavelength in the range of ca. 30 nm can be observed. Thus, the lasing wavelength of PAAzo-based DFB structures can be easily tuned just by varying the angle between the orientation direction of side groups of the LC copolymer PAAzo and the grating vector.

The longest generation wavelength was obtained for orthogonal orientation of the grating vector with respect to the substrate rubbing direction. Figure 7 shows the lasing spectra for the DFB structures of this orientation with grating periods of 255 nm (black line) and 245 nm (red line), respectively. It can be seen that in addition to the mode with an effective refractive index of 1.58 (lasing wavelength of 805 nm for the grating period of 255 nm and lasing wavelength of 776 nm

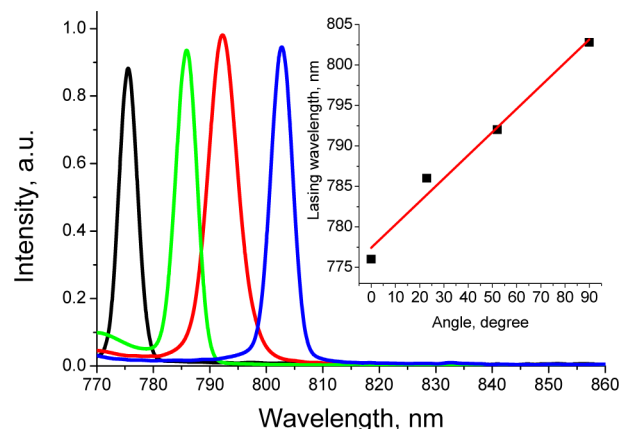


**Figure 6.** Lasing spectra of different DFB structures in PAAzo+Rh700 with a grating vector rotated with respect to the LC director by the angles 0 (black line), 38 (green line), 67 (red line), and 90 (blue line) degrees (pumping at 605 nm, film thickness 550 nm, grating period 255 nm). The inset shows the dependency of the lasing wavelength on this angle (scatters) with linear fit (red line).

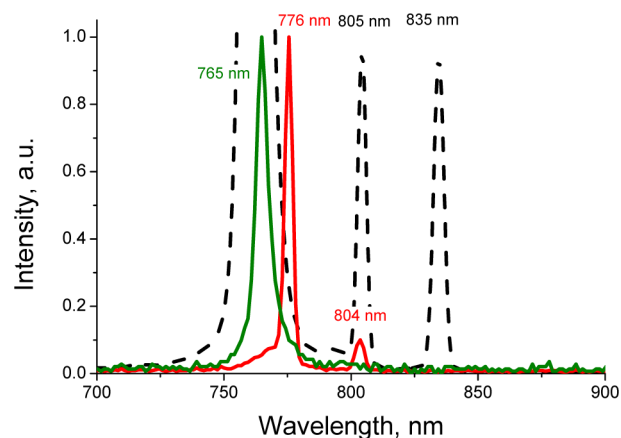


**Figure 7.** Lasing spectra of different DFB structures in PAAzo+Rh700 with grating vector orthogonal to the LC director. Pump wavelength is 605 nm; film thickness is 600 nm; the grating period is 255 nm (black line), 245 nm (red line), and 467 nm (green line).

nm for the grating period of 245 nm) another mode can be excited with an effective refractive index of 1.64 (lasing wavelength of 836 nm for the grating period of 255 nm and lasing wavelength of 804 nm for the grating period of 245 nm). This second mode was not observed in the DFB structures with grating vector parallel to the substrate rubbing direction, in which only single-mode operation was detected. It is interesting that only for such a mode was it possible to obtain laser generation for the second-order DFB structure ( $m$  is equal to 2 in eq 3) with a grating period of about 467 nm. The generation spectrum is also presented in Figure 7 (green line).

It was found that irradiation of oriented films with Ar-laser radiation, linearly polarized in a direction parallel to the rubbing direction of the substrate, prior to grating inscription shifts the lasing wavelength. This is illustrated in Figure 8 for the cases of the DFB structures written parallel (a) and orthogonal (b) to the rubbing direction. It can be seen that in the first case the lasing wavelength is increased, while in the second case the wavelength decreases. This effect can be explained by the fact that irradiation of the film with light polarized parallel to the rubbing direction reorients a part of LC domains into

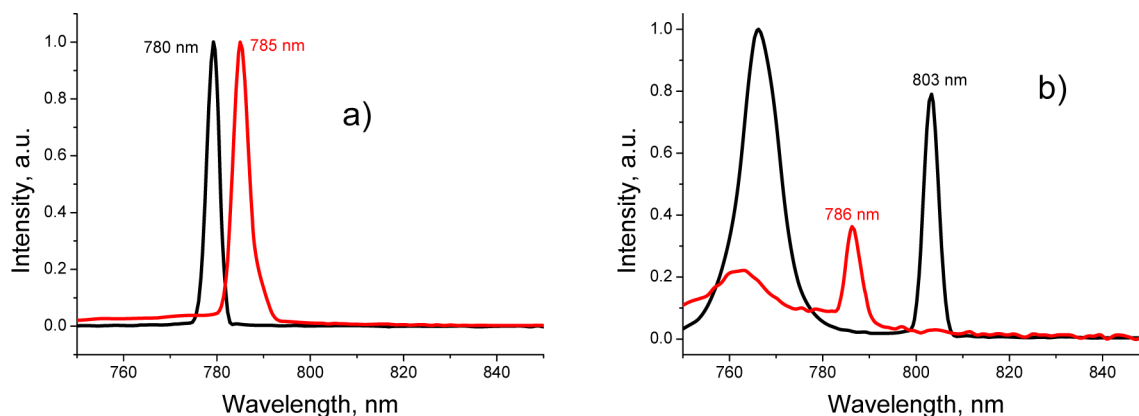


**Figure 8.** Lasing spectra of different DFB structures in PAAzo+Rh700 with grating vectors parallel to the LC director (a) and orthogonal to the LC director (b). The pumping wavelength is 605 nm, film thickness is 600 nm, grating period is 255 nm; red lines correspond to the lasing spectra for the films, which were irradiated with light linearly polarized parallel to the LC director before the gratings were recorded; black lines correspond to the lasing spectra for the films without such irradiation.

orthogonal directions. As a result, the difference between parallel orientation of the grating vector and orthogonal orientation is decreased.

The threshold of lasing was ca.  $0.2 \text{ mJ cm}^{-2}$  for the DFB structures written with the grating vector parallel to the LC director. When the gratings were recorded with their vector perpendicular to the rubbing direction, the lasing threshold was about two times higher. It is remarkable that these threshold values can be achieved even for a grating inscription time of about 1 s, while previously for other azobenzene matrices under similar intensity conditions<sup>5–7</sup> not less than 40 s long inscription has been used. The dependence of output energy on pump energy was measured for the best case (grating vector is parallel to the LC director) and is presented in Figure 9. The

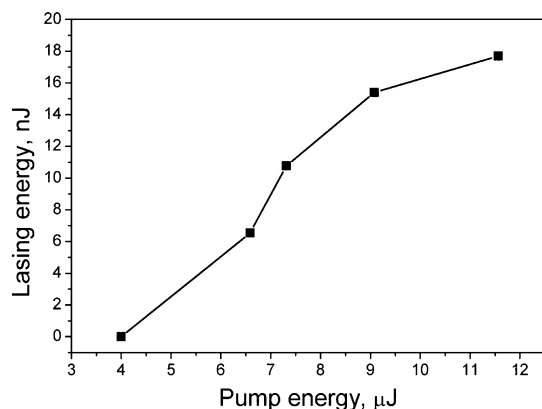


**Figure 9.** Output lasing energy versus pump energy per pulse for the DFB laser inscribed into PAAzo+Rh700 (grating vector parallel to the LC director; pumping at 605 nm, film thickness 500 nm, grating period 255 nm).

energy detected from one side of the DFB structure was 18 nJ for the pump energy of 12  $\mu\text{J}$  per pulse. This corresponds to an efficiency of generation from both sides of the DFB laser of ca. 0.3%, which is practically equal to the lasing efficiency of LDS 730 in a PAZO matrix<sup>4</sup> for the same pump energy. However, the long-term stability of the DFB laser was not particularly high. The half-lifetime was measured to be ca.  $3 \times 10^3$  pulses. The long-term decrease of pulse energy was not accompanied by a change of spectrum of the generated radiation.

Similarly to the previous investigations,<sup>6</sup> the gratings were easily overwritten with a different grating frequency, yielding a different emitting wavelength. However, while in the current case the inscription time is much shorter, the number of possible rewriting cycles is much higher. We performed a turn by turn writing of gratings with periods of 250 and 270 nm in the same film using an inscription time of 5 s. No significant change of lasing intensity was detected after 25 cycles of rewriting. A sufficiently large number of possible rewriting cycles can be expected when the inscription time is decreased to 1 s.

**Lasing in Oriented Films with Other NIR Dyes.** An application of other NIR laser dyes (Rhodamine 800, LDS 798, and LDS 730) also led to a laser device with a somewhat higher lasing threshold of  $2\text{--}5 \text{ mJ cm}^{-2}$ . The lasing spectra for these dyes are shown in Figure 10a. With the dye LDS 798 it was possible to extend the tuning range to 883 nm (Figure 10b).

When the data for all dye formulations with different grating frequencies (with the grating vector parallel to the rubbing direction) were plotted (Figure 10c), the same value of refractive index of ca. 1.52 was yielded. All dye combinations together allowed the tuning range from 760 to 883 nm.

## CONCLUSION

For the first time an azobenzene-containing LC polymer was applied as a medium for DFB lasers based on polarization gratings. It was shown that the LC azobenzene-containing polymer matrix has noticeable advantages, such as a very short time for grating recording (about one second at moderate light intensity) and the possibility to easily rewrite or erase a polarization grating. Using the different NIR laser dyes together with various periods of orientation gratings allows one to change the lasing wavelength from 760 nm to 883 nm. In addition, the possibility of lasing wavelength tuning by not only variation of the grating period but also by simple changing the angle between the LC director (direction of orientation of side groups of the LC polymer) and the grating vector was demonstrated. This new approach allows one to alter the emission wavelength in the range of 30 nm.

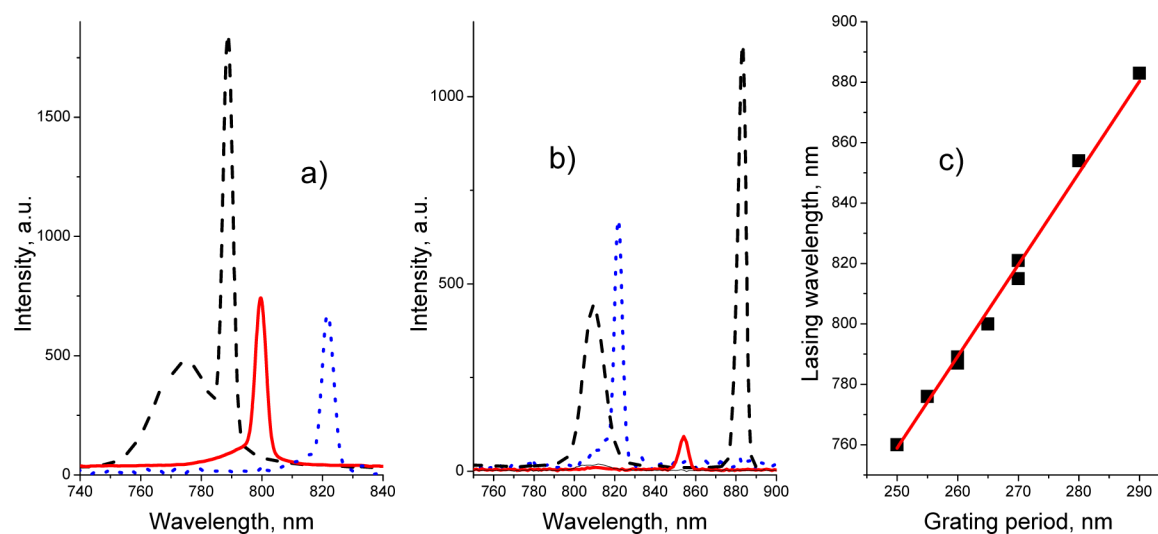


**Figure 10.** Lasing spectra of different DFB structures in the systems based on the LC polymer PAAzo containing different NIR laser dyes: (a) LDS 730, period 260 nm (dashed line); LDS 798, period 265 nm (solid line); Rhodamine 800, period 270 nm (dotted line); (b) tuning of lasing spectra in formulation with LDS 798, periods 270–290 nm; (c) dependency of emitted wavelength on the grating period for all lasers with different dyes and grating periods (with the grating vector parallel to the rubbing direction).

## ■ ASSOCIATED CONTENT

### 📄 Supporting Information

In Figure S1 the image of a sample after grating inscription obtained with atomic force microscopy is presented. The figure proves the absence of SRG. This material is available free of charge via the Internet at <http://pubs.acs.org>.

## ■ AUTHOR INFORMATION

### Corresponding Authors

\*E-mail: [lengold57@gmail.com](mailto:lengold57@gmail.com).

\*E-mail: [lisinetskii@gmail.com](mailto:lisinetskii@gmail.com). Phone: (+49) 3375508461.

### Present Address

#Plasmachem GmbH, Rudower Chaussee 29, 12489 Berlin, Germany.

### Notes

The authors declare no competing financial interest.

## ■ ACKNOWLEDGMENTS

This research was supported by the Alexander von Humboldt Foundation and the Russian Foundation of Fundamental Research (13-03-00648\_a, 13-03-12456\_ofi\_m, 13-03-12071\_ofi\_m).

## ■ REFERENCES

- (1) Lu, M.; Choi, S. S.; Wagner, C. J.; Eden, J. G.; Cunningham, B. T. Label free biosensor incorporating a replica-molded, vertically emitting distributed feedback laser. *Appl. Phys. Lett.* **2008**, *92*, 261502.
- (2) Yang, Y.; Turnbull, G. A.; Samuel, I. D. W. Sensitive explosive vapor detection with polyfluorene lasers. *Adv. Funct. Mater.* **2010**, *20*, 2093–2097.
- (3) Goldenberg, L. M.; Lisinetskii, V.; Gritsai, Y.; Stumpe, J.; Schrader, S. Single step optical fabrication of a DFB laser device in fluorescent azobenzene-containing materials. *Adv. Mater.* **2012**, *24*, 3339–3343.
- (4) Goldenberg, L. M.; Lisinetskii, V.; Gritsai, Y.; Stumpe, J.; Schrader, S. First observation of DFB lasing in polarization gratings written in azobenzene film. *Laser. Phys. Lett.* **2013**, *10*, 085804–085808.
- (5) Goldenberg, L. M.; Lisinetskii, V.; Schrader, S. Azobenzene lasers tuned over a 200 nm range. *Adv. Opt. Mater.* **2013**, *1*, 527–533.

(6) Goldenberg, L. M.; Lisinetskii, V.; Schrader, S. Stable lasing in azobenzene polyelectrolyte with polarization gratings as distributed feedback. *Adv. Opt. Mater.* **2013**, *1*, 768–775.

(7) Goldenberg, L. M.; Lisinetskii, V.; Schrader, S. Stable and efficient thin layer DFB lasers based on side-chain azobenzene polymers. *Adv. Opt. Mater.* **2014**, *2*, 286–291.

(8) Yager, K. G.; Barrett, C. J. Light-Induced Nanostructure Formation Using Azobenzene Polymers, Chapter 8. In *Polymeric Nanostructures and Their Applications*; Nalwa, H. S., Ed.; American Scientific Publishers, 2006.

(9) *Smart Light-Responsive Materials: Azobenzene-Containing Polymers and Liquid Crystals*; Zhao, Y.; Ikeda, T., Eds.; Wiley & Sons: Hoboken, NJ, USA, 2009.

(10) Nikolova, L.; Ramanujam, P. S. *Polarization Holography*; Cambridge Academic Press: Cambridge, UK, 2009.

(11) Goldenberg, L. M.; Kulikovskiy, L.; Kulikovskaya, O.; Tomczyk, J.; Stumpe, J. Very efficient surface relief holographic materials based on azobenzene-containing epoxy resins cured in films. *J. Mater. Chem.* **2010**, *20*, 9161–9171.

(12) Okano, K.; Shishido, A.; Ikeda, T. An azotolane liquid-crystalline polymer exhibiting extremely large birefringence and its photo-responsive behavior. *Adv. Mater.* **2006**, *18*, 523–527.

(13) Lachut, B. L.; Maier, S. A.; Atwater, H. A.; de Dood, M. J. A.; Polman, A.; Hagen, R.; Kostromine, S. Large spectral birefringence in photoaddressable polymer films. *Adv. Mater.* **2004**, *16*, 1746–1750.

(14) Bruder, F.-K.; Hagen, R.; Rölle, T.; Weiser, M.-S.; Fäcke, T. From the surface to volume: concepts for the next generation of optical–holographic data-storage materials. *Ang. Chem., Int. Ed.* **2011**, *50*, 4552–4573.

(15) Priimagi, A.; Shevchenko, A. Azopolymer-based micro- and nanopatterning for photonic applications. *J. Polym. Sci. Polym. Phys.* **2014**, *52*, 163–182.

(16) Yu, H.; Kobayashi, T. In *Azobenzene-Containing Materials for Hologram, Holograms - Recording Materials and Applications*; Naydenova I., Ed.; InTech, 2011.

(17) Yu, H.; Ikeda, T. Photocontrollable liquid-crystalline actuators. *Adv. Mater.* **2011**, *23*, 2149–2180.

(18) Yu, H. Recent advances in photoresponsive liquid crystalline polymers containing azobenzene chromophores. *J. Mater. Chem. C* **2014**, *2*, 3047–3054.

(19) Zhang, X.; Zhang, J.; Sun, Y.; Yang, H.; Yu, H. Erasable thin-film optical diode based on a photoresponsive liquid crystal polymer. *Nanoscale* **2014**, *6*, 3854–3860.



- (20) Garcia, T.; Larios-Lopez, L.; Julia Rodriguez-Gonzalez, R.; Martinez-Ponce, G.; Solano, C.; Navarro-Rodriguez, D. Liquid-crystalline polymers bearing phenylene(azobenzene) moieties substituted with an electron-donor or electron-acceptor lateral group. Synthesis, mesomorphic behavior and photo-induced isomerisation. *Polymer* **2012**, *53*, 2049–2061.
- (21) Lachut, B. L.; Maier, S. A.; Atwater, H. A.; de Dood, M. J. A.; Polman, A.; Hagen, R.; Kostromine, S. Large spectral birefringence in photoaddressable polymer films. *Adv. Mater.* **2004**, *16*, 1746–1750.
- (22) Bobrovsky, A.; Shibaev, V. Polarised light-induced orientation and reorientation processes and unexpected 'memory effect' in side-chain azobenzene-containing LC polymers. *Liq. Cryst.* **2012**, *39*, 339–345.
- (23) Shishido, A. Rewritable holograms based on azobenzene-containing liquid-crystalline polymers. *Polym. J.* **2010**, *42*, 525–533.
- (24) Shibaev, V.; Bobrovsky, A.; Boiko, N. Photoactive liquid crystalline polymer systems with light-controllable structure and optical properties. *Prog. Polym. Sci.* **2003**, *28*, 729–836.
- (25) Ichimura, K. Photoalignment of liquid-crystal systems. *Chem. Rev.* **2000**, *100*, 1847–1873.
- (26) Bobrovsky, A.; Ryabchun, A.; Medvedev, A.; Shibaev, V. Ordering phenomena and photoorientation processes in photochromic thin films of LC chiral azobenzene-containing polymer systems. *J. Photochem. Photobiol. A: Chem.* **2009**, *206*, 46–52.